ISBN: 978-3-95450-227-1 ISSN: 2673-5490 doi:10.18429/JACoW-IPAC2022-TUPOPT051

RECONSTRUCTION AND BEAM-TRANSPORT STUDY OF THE cERL DUMP LINE FOR HIGH-POWER IR-FEL OPERATION

N. Nakamura†, Y. Tanimoto, N. Higashi, K. Harada, M. Shimada, T. Uchiyama, T. Nogami, A. Ueda, S. Nagahashi, T. Obina, R. Takai, H. Sagehashi, K. Nigorikawa, O. Tanaka, R. Kato, H. Sakai, High Energy Accelerator Research Organization, Tsukuba, Japan

Abstract

Infrared (IR) SASE-FEL emission was successfully generated for macro pulses of about 1 μs with the maximum repetition rate of 5 Hz at the cERL. In the future, high-power FEL operation will be planned to increase electron bunches drastically with energy recovery. Therefore, the dump line was redesigned and reconstructed to increase the momentum acceptance and to improve the magnet system for avoiding serious beam loss in the high power FEL operation. Furthermore, the first beam-transport study was performed by transporting the beam directly from the injector to the beam dump through the reconstructed dump line. In this paper, we present the reconstructed dump line and the beam-transport study. The new dump line can be a model for dump lines of high-power ERL-FELs.

INTRODUCTION

A significant FEL pulse energy was generated at the cERL IR-FEL [1] in Burst mode where a macro pulse of about 1 μs is repeated at the maximum frequency of 5 Hz. In the next step, high-power FEL operation in CW mode should be carried out with energy recovery by increasing electron bunches drastically. However, momentum spread of the electron beam increases due to the FEL emission and the space charge effects and may cause serious beam loss by exceeding the momentum acceptance of the cERL downstream of the FEL. Therefore, we reconstructed the dump line in Autumn 2020 to greatly increase the momentum acceptance and to improve the magnet system for more flexible beam control. Then we carried out the beam-transport study of the new dump line in March 2021 by injecting the beam directly from the injector without passing the recirculation loop.

MOMENTUM ACCEPTANCE

Beam loss must be efficiently suppressed in the high-power FEL operation at the cERL [2] in terms of radiation safety and machine protection, because the beam current is much increased in CW mode as compared that in Burst mode. The electron beam can have large momentum spread due to the FEL emission and the longitudinal space charge effects and cause significant beam loss at the dispersion sections by exceeding the apertures of the beam ducts. To avoid it, the momentum acceptance downstream of the FEL must be sufficiently large compared to the momentum spread of the electron beam. The main dispersion sections downstream of the FEL are the 2nd arc and the dump line as shown in Fig. 1. In the FEL operation, we have so far used Burst mode, where the electron beam is dumped without energy recovery at the movable dump before the dump line. In the high-power FEL operation, the high-current beam is decelerated in the main linac for energy recovery and transported to the beam dump through the dump line.

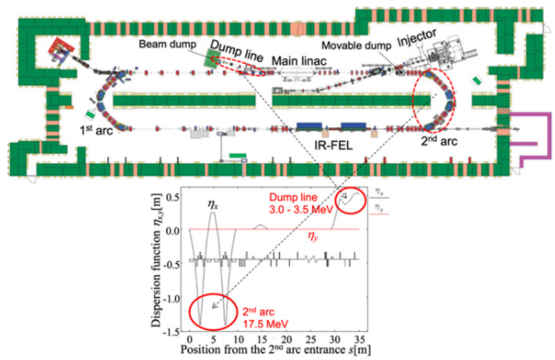

Figure 1: Layout of the cERL including the two dispersive sections, the 2nd arc and dump line, downstream of the IR-FEL with the dispersion functions.

The momentum acceptance is defined with the maximum dispersion function $\eta_{x,\,max}$ and the beam-duct aperture A_x in the dispersion section by the following equation.

$$\left(\frac{\Delta p}{p}\right)_{MA} = \frac{A_x}{\eta_{x,max}} \quad (1)$$

In Eq. (1), the effect of the betatron beam size is neglected for simplicity.

In the cERL, two beams with different momenta pass for energy recovery between the exit of the injector and the entrance of the dump line. In the injection and dump chicanes, the lower-momentum beam is deflected by 16 degrees for injection and dump and the higher-momentum beam makes closed bump orbits. The ratio of the lower and higher momenta must be less than 1/5 in order that the higher-momentum beam does not hit the beam ducts in the injection and dump chicanes. Therefore, the beam energy at the dump line must be 3.5 MeV or lower when the beam energy in the recirculation loop including the FEL and the 2nd arc is set to 17.5 MeV. Table 1 shows the parameters of the two dispersion sections downstream of the IR-FEL, the 2nd arc and the dump line before and after the reconstruction. The values within parentheses in the table are the momentum acceptances of the dump line normalized by the momentum at the 2nd arc for comparing the momentum acceptances of the different momenta. The normalized momentum acceptance before the

† noro.nakamura@kek.jp.

ISBN: 978-3-95450-227-1 ISSN: 2673-5490 doi:10.18429/JACoW-IPAC2022-TUPOPT051

reconstruction is significantly smaller than that of the 2nd arc. This means that beam loss at the dump line can be the largest in the cERL. Therefore, we decided to redesign and reconstruct the dump line for the purpose of improving the normalized momentum acceptance up to that of the 2nd arc at least. The parameter values for the dump line after the reconstruction are also shown in Table 1 and described in detail in the next section.

Table 1: Parameters of the 2nd Arc and the Dump Line Before and After Reconstruction

2nd arc	
Beam energy	17.5 MeV
Aperture	35 mm
Maximum dispersion	1.4 m
Momentum acceptance	2.50 %
Dump line before reconstruction	
Beam energy	3.53 MeV
Aperture	42.45 mm
Maximum dispersion	0.523 m
Momentum acceptance	8.12 % (1.62# %)
Dump line after reconstruction	
Beam energy	3.53 MeV
Aperture	48.70 mm
Maximum dispersion	0.341 m
Momentum acceptance	14.28 % (2.86# %)

Normalized by the beam momentum at the 2nd arc

RECONSTRUCTION OF DUMP LINE

The layout of the dump line before and after the reconstruction is shown in Fig. 2.

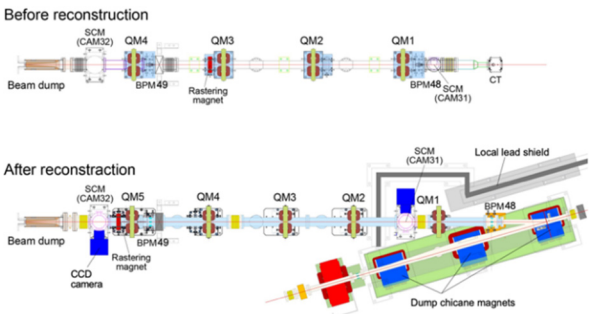

Figure 2: Layout of the cERL dump line before (upper) and after (lower) reconstruction. The beam line with the dump chicane, the local lead shield and the CCD cameras for the screen monitors (SCMs) are the same before and after the reconstruction and omitted in the upper figure.

In the reconstruction, the aperture of the circular beam duct downstream of the first quadrupole magnet QM1 in the dump line was increased from 42.45 to 48.70 mm in inner radius. The beam duct is made of stainless steel with 2.1-mm thickness. The maximum aperture was limited by the bore radius of the quadrupole magnets (51 mm) in the dump line. Furthermore, the quadrupole magnet QM1 was moved as upstream as possible (40 cm upstream) and as a result the maximum dispersion function was reduced from 0.523 to 0.341 m as shown in Table 1. The normalized momentum acceptance of the dump line was increased from 1.62 to 2.86 %, which is larger than that of the 2nd arc.

The number of the quadrupole magnets in the dump line was increased from four to five to control the beam more flexibly. QM1, QM3 and QM5 have sub-coils for tuning the horizontal and vertical beam orbits. The rastering magnet [3], which scans the beam position horizontally and vertically for reducing the thermal load on the beam dump, was also moved from just after QM3 to just after QM5 so that the beam position and size at the beam dump should not depend on field strength of the quadrupole magnet. The layout of the rastering magnet and the beam dump is shown in Fig. 3. The distance between them is 697 mm. The rastering image at the beam dump is estimated by using the beam position movement at the screen monitor CAM32, which is placed at 216 mm from the rastering magnet. The screen monitors CAM31 and CAM32 with the half aperture of 50 mm were reused in the new layout. The beam position monitor BPM48 with the aperture of 42.5 mm was reused and BPM49 was renewed to increase the half aperture to 50 mm. The current transformer (CT) was removed.

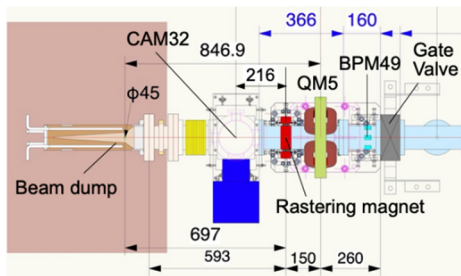

Figure 3: Layout of the rastering magnet and the beam dump.

BEAM-TRANSPORT STUDY

The first beam-transport study of the reconstructed dump line was carried out on March 18 in 2021. The beam line used for the study and the direction of the beam transport are shown in Fig. 4.

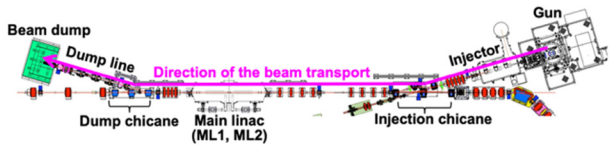

Figure 4: Layout of the used beam line and the beam direction in the beam-transport study.

In the study, the electron beam with the bunch charge of 60 pC was operated in Burst mode, which was the same as that of the IR-FEL operation. The injection energy in front of the main linac with two superconducting cavities, ML1 and ML2, is 5 MeV and the used parameters from the electron gun to the entrance of ML2 were the same as those of the FEL operation carried out in March 2021. The beam energy is 10 MeV between ML1 and ML2. The beam was

ISBN: 978-3-95450-227-1 ISSN: 2673-5490 doi:10.18429/JACoW-IPAC2022-TUPOPT051

decelerated by using the ML2 cavity and transported to the dump line in the beam-transport study, though it was accelerated to about 17.5 MeV in the FEL operation.

The 10-MeV beam between the ML1 and ML2 cavities was decelerated to 3.5 MeV in the ML2 cavity. First the RF amplitude and phase of the ML2 cavity were adjusted to decelerate the beam on crest to 3.5 MeV. Figure 5a shows the beam profiles measured by CAM31 and CAM32. The measured horizontal and vertical beam sizes in rms were 3.6 and 2.5 mm at CAM 31 and 3.4 and 1.1 mm at CAM32. Next the RF phase of the ML2 cavity was shifted by 30 degrees with keeping the beam energy at 3.5 MeV by the RF amplitude. In this off-crest deceleration by the ML2 cavity, the momentum spread became very large compared to that of the on-crest deceleration. This experimentally simulated an electron beam with a large momentum spread caused by the IR-FEL emission and/or the space charge effects. The horizontal beam size greatly increased to about 12 mm at CAM31 ($\eta_x \sim 0.28$ m) as shown in Fig. 5b. However, the beam sizes could be well controlled within a few mm at CAM32 by the new magnet system in the dump line.

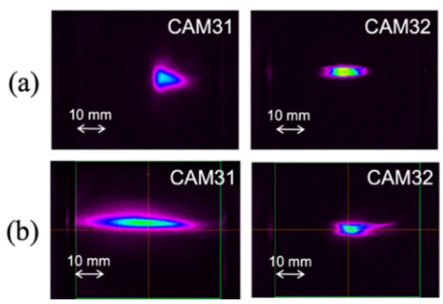

Figure 5: Profiles of the 3.5-MeV beam observed at CAM31 and CAM32 for the (a) on-crest and (b) off-crest deceleration of the ML2 cavity.

The beam was transported to the beam dump while the beam position was transversely being scanned by the rastering magnet. Figures 6a and 6b show traces of the beam positions measured at CAM32 with the rastering magnet on for on-crest and off-crest deceleration of the ML2 cavity. The rastering circle size in this study was set to 6.6 – 6.8 mm at CAM32 in diameter and hence 21 – 22 mm at the entrance of the beam dump. The rastering frequency was set to 10 Hz, at which the beam position filled the rastering circle twice and returned to the initial position.

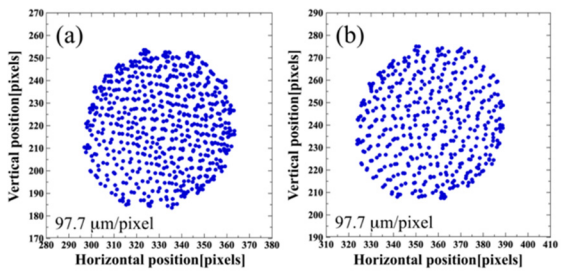

Figure 6: Beam position movement by the rastering magnet at CAM32 for the (a) on-crest and (b) off-crest deceleration of the ML2 cavity.

Figure 7 shows the betatron and dispersion functions, the momentum spread and beam sizes in rms from the ML2 cavity to the beam dump for the off-crest deceleration of the ML2 cavity. The optics design and beam simulation were performed by using the simulation code Elegant [4] with the initial distribution at the center of the main linac calculated by GPT [5]. The longitudinal space charge (LSC) effects and coherent synchrotron radiation (CSR) effects were taken into consideration in the Elegant simulation. The momentum spread reaches to about 3.4 % and the maximum horizontal beam size exceeds 11 mm. As shown in Fig. 7d, the new magnet system of the dump line can well adjust both horizontal and vertical beam sizes to about 2 mm at the beam dump, which is suitable for the rastering system. The simulation result is roughly consistent with the measurement result of the beam-transport study.

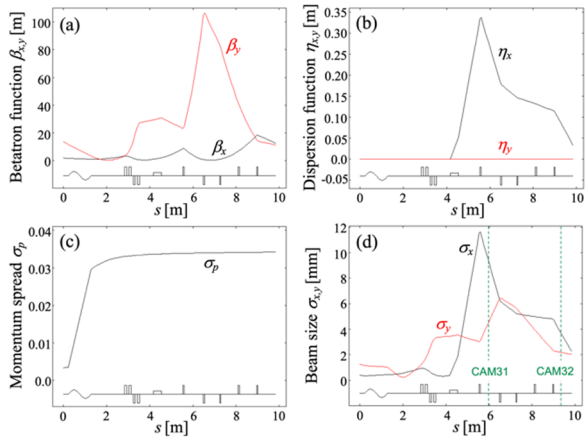

Figure 7: (a) Betatron and (b) dispersion functions, (c) momentum spread and (d) beam sizes along the dump line from the ML2 cavity to the beam dump calculated for the off-crest deceleration.

SUMMARY

We summarize our presentation on the reconstructed dump line and the beam-transport study below.

- The largest beam loss had a possibility of occurring at the dump line in the high-power IR-FEL operation at the cERL, because the dump line had the minimum normalized momentum acceptance.
- The dump line was reconstructed in Autumn 2020 to improve the momentum acceptance by 76 % and to enhance flexibility of the magnet system in beam control.
- The first beam-transport study was done in March 2021 and as a result the beam was successfully transported with rastering on to the beam dump through the reconstructed dump line.
- The new cERL dump line is expected to well work in the high-power FEL operation and to serve as a model for dump lines of high-power ERL-FELs.

ISBN: 978-3-95450-227-1 ISSN: 2673-5490 doi:10.18429/JACoW-IPAC2022-TUPOPT051

ACKNOWLEDGEMENTS

We would like to thank all the members of the cERL IR-FEL team. This work is supported by a NEDO project "Development of advanced laser processing with intelligence based on high-brightness and high-efficiency laser technologies."

REFERENCES

[1] Y. Honda *et al*., "Construction and commissioning of mid-infrared self-amplified spontaneous emission free-electron laser at compact energy recovery linac", *Rev. Sci. Instrum*., vol. 92, no. 11, p. 113101, 2021.

[2] M. Akemoto *et al*., "Construction and commissioning of the compact energy-recovery linac at KEK", *Nucl. Instrum. Methods*, vol. A877, pp. 197-219, 2018.

[3] K. Harada *et al*., "Rastering system with interlock for the beam dump of cERL", in *Proc. 13th Annual Meeting of Particle Accelerator Society of Japan*, Chiba, Japan, Aug. 2016, pp. 585-588 (*in Japanese*).

[4] M. Borland, "ELEGANT: A flexible SDDS-compliant code for accelerator simulation", *Advanced Photon Source,* LS-287, p. 2000, Sep. 2000. doi:10.2172/761286

[5] O. A. Tanaka, N. Higashi, and T. Miyajima, "Injector Optimization for the IR-FEL Operation at the Compact ERL at KEK", in *Proc. IPAC'21*, Campinas, Brazil, May 2021, pp. 4531-4534. doi:10.18429/JACoW-IPAC2021-FRXB07